Title: Chronic high-sugar diet in adulthood protects *Caenorhabditis elegans* from 6-OHDA induced dopaminergic neurodegeneration

Authors and Affiliation: Katherine S. Morton[1], Jessica H. Hartman[1,2], Nathan Heffernan[1], Ian T. Ryde[1], Isabel W. Kenny-Ganzert [3], Lingfeng Meng[1], David R. Sherwood[3], Joel N. Meyer[1]

[1]Nicholas School of Environment, Duke University

[2]Biochemistry and Molecular Biology, Medical University of South Carolina

[3]Department of Biology, Duke University

Declarations: The authors declare no competing interests

Abstract

Background: Diets high in saturated fat and sugar, termed 'western diets', have been associated with several negative health outcomes, including increased risk for neurodegenerative disease. Parkinson's Disease (PD) is the second most prevalent neurodegenerative disease and is characterized by the progressive death of dopaminergic neurons in the brain. We build upon previous work characterizing the impact of high sugar diets in *Caenorhabditis elegans* to mechanistically evaluate the relationship between high sugar diets and dopaminergic neurodegeneration.

Results: Non-developmental high glucose and fructose diets led to increased lipid content and shorter lifespan and decreased reproduction. However, in contrast to previous reports, we found that non-developmental chronic high-glucose and high-fructose diets did not induce dopaminergic neurodegeneration alone and were protective from 6-hydroxydopamine (6-OHDA) induced degeneration. Neither sugar altered baseline electron transport chain function, and both increased vulnerability to organism-wide ATP depletion when the electron transport chain was inhibited, arguing against energetic rescue as a basis for neuroprotection. The induction of oxidative stress by 6-OHDA is hypothesized to contribute to its pathology, and high sugar diets prevented this increase in the soma of the dopaminergic neurons. However, we did not find increased expression of antioxidant enzymes or glutathione levels. Instead, we found evidence suggesting alterations to dopamine transmission that could result in decreased 6-OHDA uptake.

Conclusion: Our work uncovers a neuroprotective role for high sugar diets, despite concomitant decreases in lifespan and reproduction. Our results support the broader finding that ATP depletion alone is insufficient to induce dopaminergic neurodegeneration, whereas increased neuronal oxidative stress may drive degeneration. Finally, our work highlights the importance of evaluating lifestyle by toxicant interactions.

Keywords:

Glucose, Fructose, Neurodegeneration, Oxidative Stress, C. elegans

65 Background:

66 In 2019 the average American consumed 50.0 g (190 calories) of refined cane or beet sugar and
67 29.3 g (111 calories) of high-fructose corn syrup per day in addition to other added caloric sweeteners
68 and naturally occurring sugars (1). Despite a small 0.71% decrease in caloric sweetener consumption
69 since 2016, this still often exceeds the World Health Organization recommendation of less than 10% of
70 total caloric intake (2). Glucose and fructose are the most consumed sugars, as the majority of sugar
71 intake in the United States comprises refined cane or beet sugar, high-fructose corn syrup, and foods
72 naturally containing glucose and fructose (3). Referred to as high-glycemic-index diets for their
73 propensity to raise blood glucose levels, high sugar diets have been linked to the increase in obesity with
74 particularly strong evidence for the consumption of sugary beverages (4).

75 Obesity is defined as a body mass index (BMI) greater than 30 and is a non-monolithic disease
76 caused by metabolic, genetic, socioeconomic, and environmental factors. It doubled in prevalence in
77 more than 70 countries between 1980 and 2015 and is epidemiologically linked to the increased
78 prevalence of type 2 diabetes, cardiovascular diseases, some neurodegenerative diseases, and surgical
79 complications including infections (5, 6). In one such neurodegenerative disease, Parkinson's disease
80 (PD), it has been reported that patients show higher total sugar and added sugar consumption than
81 healthy controls (7). Despite evidence of higher disease-concurrent intake in diagnosed individuals, it is
82 less clear how sugar diets influence the onset of PD (8).

83 PD is a late-onset neurodegenerative disorder characterized by loss of function and death in the
84 dopaminergic neurons of the substantia nigra region of the brain. PD impacts 1-3% of the global
85 population over age 65. Oxidative stress and mitochondrial dysfunction have both been identified as
86 potential causes or critical steps in the pathology of the disorder (9). Epidemiological studies
87 consistently find relationships between blood glucose levels, insulin intolerance, and PD. Though the

88 causal nature is unclear, increased blood glucose levels have been identified in drug-naïve patients and
89 those showing cognitive decline (10), and elevated blood glucose is a predictor of cognitive decline (11).
90 Increased added sugar intake has been associated with increased frequency of developing PD and
91 greater symptom severity and medication requirements post diagnosis (12).These same studies and
92 others have further found that decreased levels of insulin and increased insulin resistance were
93 associated with cognitive decline in PD patients (10, 11, 13). It has not been clearly established if
94 increased sugar intake and elevated blood glucose are causal or secondary to decreased insulin levels
95 and sensitivity to insulin.

96 To expand understanding of the complex relationship between high sugar diets, obesity, and
97 susceptibility to dopaminergic neurodegeneration, we turned to the nematode *Caenorhabditis elegans*.
98 *C. elegans* has been widely used as a model in biomedical research in general and to explore the impacts
99 of high-sugar diets in particular, because of its high genetic homology to humans, short life cycle, and
100 conservation of key pathways including insulin signaling (14). *C. elegans* fed high-glucose diets generally
101 demonstrate slower growth, decreased reproduction, shortened lifespan, neuronal and mitochondrial
102 dysfunction, decreased anoxia survival, and increased oxidative stress (15-19). High-fructose diets,
103 though less explored, have been shown to decrease lifespan and health span, induce mitochondrial
104 swelling, and decrease anoxia survival of worms (19, 20).

105 *C. elegans* has also been employed for studies of PD. Possessing 8 dopaminergic neurons and
106 high genetic tractability, several transgenics have been generated to assist with visualization of
107 dopamine neuron morphology (21, 22). High glucose exposure studies in *C. elegans* showed increased
108 susceptibility to organophosphate pesticide-induced neurodegeneration in dopaminergic, GABAergic,
109 and cholinergic neurons (17, 18, 23). These studies, however, were mostly performed with acute,
110 developmental exposures to glucose.

111 Here, we present evidence from worms fed chronic, not acute, 100 mM D-glucose or fructose
112 from day 1-day 5 of adulthood on the mechanistic relationships between high-sugar diets and
113 dopaminergic neurodegeneration. With this strategy, we have avoided the potential for confounding
114 effects of bioenergetic remodeling resulting from developmental mitochondrial stress (24-28). Doses
115 were selected to closely match the large body of literature in *C. elegans* studying high sugar diets, in
116 which 100 mM consistently produces clear effects but is non-lethal (Table 1). To improve upon the
117 common use of decreased fluorescence of the cell bodies within the cephalic (CEP) neurons in the head
118 of the worm as a proxy for degeneration, we employ a neurodegeneration scoring methodology with
119 improved ability to detect subtle changes to the neuronal processes. We not only assess whether high
120 sugar diets induce dopaminergic neurodegeneration, but whether they enhance susceptibility to the
121 canonical dopaminergic neurotoxicant 6-hydroxydopamine (6-OHDA). Upon entering the cell, 6-OHDA
122 increases oxidative stress partly through auto-oxidation, and partly through inhibition of mitochondrial
123 electron transport chain Complexes I and IV, resulting in decreased ATP levels, akin to two other PD
124 toxicant model toxicants, rotenone and MPP+ (29). Utilizing this method, we report that chronic, non-
125 developmental high glucose or high fructose diets resulted in neuroprotection from 6-OHDA exposure.
126 The impact of 6-OHDA on redox state, not its effect on ATP levels, was abrogated by high sugar,
127 suggesting that redox alterations, not energetic alterations, underlie the dopaminergic neurotoxicity of
128 6-OHDA in *C. elegans*. In absence of alterations to glutathione levels, redox tone, and antioxidant
129 enzyme expression, we suggest altered dopamine neurotransmission leads to decreased 6-OHDA uptake
130 and prevents toxicity.

131 Results:

132 **Non-developmental high sugar diets decrease lifespan and fecundity while increasing adiposity**

133 *C. elegans* has been used extensively to evaluate the impacts of dietary paradigms on lifespan and
134 reproduction. In the case of high sugar diets, previous work in *C. elegans* has focused largely on
135 exposures beginning in early development. To discern how non-developmental (adult) glucose and
136 fructose exposures impact key biological functions, and permit comparison to previously published
137 developmental exposure studies, we first evaluated the impact of our adult exposure paradigm on
138 adiposity, lifespan, and fecundity. In concurrence with the effects observed with developmental sugar
139 exposures, worms transferred as young adults to nematode growth media (NGM) plates supplemented
140 with 100 mM glucose or 100 mM fructose show increased lipid accumulation represented by an 85.6%
141 and 46.2% increase in fluorescence intensity of an mCherry::mdt-28 fusion protein localized primarily to
142 lipid droplets (Fig 1A). Increased lipid stores were particularly concentrated throughout the intestine,
143 around the vulva, and to a lesser extent in the head. The effect was more intense in glucose fed worms
144 than fructose fed worms (Fig 1B). Similarly, and again in agreement with observations from
145 developmental exposures, worms fed glucose and fructose had a modest decrease in their average
146 brood size from 297.7±7.9 eggs per worm to 247.9±7.9 and 272.7±4.8 respectively (Fig 1C). Beyond total
147 brood size, the time course of egg laying was altered such that both high sugar diets caused egg laying to
148 be distributed more evenly over days 1-3 of adulthood as opposed to most being laid the first 2 days
149 with a sharp decrease on the third (Fig 1D), which is the typical pattern on control plates. Finally, both
150 sugars led to a significantly decreased median lifespan (Fig 1E), with a greater decrease on fructose (6
151 days shorter than control diet) than glucose (2 days shorter).

152 **High sugar diets protect from 6-OHDA induced dopaminergic neurodegeneration**

153 To define the role of high sugar diets in age-related and toxicant-induced neurodegeneration, we
154 compared dendritic degeneration in worms exposed to high sugar diets throughout reproductive
155 adulthood and subsequently exposed to either 25 mM or 50 mM 6-hydroxydopamine (6-OHDA). 6-
156 OHDA is a well-validated dopaminergic neurotoxicant transported into the dopaminergic neurons via

157 the DAT-1 transporter. The CEP neurons in *C. elegans* are easily visualized within the head of the worm
158 and have a well characterized damage phenotype including dendritic blebbing and breaking (21, 22, 30-
159 32). Using a qualitative scale in which increasing score represents increasing damage, we found that high
160 sugar diets did not increase age related neurodegeneration. In response to both 25 mM and 50 mM 6-
161 OHDA exposure, glucose and fructose fed worms were protected from neurodegeneration, with fewer
162 instances of broken and fully deteriorated sections of dendrite (Fig 2A, 2B).

163 **Neuroprotection by high sugar diets is not explained by alterations in mitochondrial amount or**
164 **morphology**

165 Next, we worked to understand the mechanism for the observed glucose and fructose
166 neuroprotection. As the 6-OHDA exposure paradigm is acute (one hour), we reasoned that the
167 mechanism of protection resulting from the chronic high sugar diet must be present when the exposure
168 begins. Both high glucose and high fructose diets have been previously associated with increased
169 mitochondrial swelling and fragmentation (20, 33). Increases or decreases in mitochondrial fission and
170 fusion dynamics are vital to cellular response to dietary and toxicant exposures (34, 35). Mitochondrial
171 fission is required for the increase in reactive oxygen species and induction of cell death by high glucose
172 diets in some cell types (36). Therefore, we evaluated mitochondrial morphology and number in the CEP
173 neuron dendrites and mitochondrial area in muscle cells to determine if clear differences in
174 mitochondrial dynamics were present prior to 6-OHDA exposure. No differences were apparent in the
175 muscle cell mitochondrial area (SFig 1) or in neuronal cell mitochondrial number (Fig 3A); however, high
176 glucose diets altered mitochondrial morphology within the CEP neurons (Fig 3B-3D). In CEP neurons,
177 high glucose diets resulted in small but significant elongation of the mitochondria from 1.832±0.04
178 micrometers to 2.005±0.05 micrometers in length (Fig 3A-B). Similarly, the maximum length of
179 mitochondria increased from 3.98±0.11 to 4.50±0.16 (Fig 3C). This resulted in an increase of total
180 mitochondrial length per dendrite from 16.45±0.32 micrometers to 18.64±0.45 micrometers (Fig 3D).

181 However, high-fructose diets did not result in any significant alterations to mitochondrial number or
182 morphology within the dendrites, indicating that even if glucose-mediated increased mitochondrial
183 length contributed to protection from 6-OHDA, fructose's protective effect could not be explained by
184 this mechanism. Continuing to assess mitochondrial mechanisms that could confer protection, we
185 moved to evaluate cellular and organismal bioenergetics.

186 **High sugar diets do not rescue ATP depletion caused by electron transport chain inhibition**

187 It has been theorized that ATP depletion may incite a negative feedback loop resulting in and enhancing
188 neurodegeneration (37, 38). Therefore, we next assessed whether the high sugar diets protected from
189 dopaminergic neurodegeneration by improving energetics at baseline, or upon challenge. On an
190 organismal level, we assessed mitochondrial bioenergetic function by whole worm respirometry. We
191 found a small increase in basal oxygen consumption rate (SFig 2); however, this is accounted for by
192 larger worm size. After accounting for worm size, we found no alterations to electron transport chain
193 function or non-mitochondrial oxygen consumption (Fig 4A). We also assessed whole-worm ATP levels
194 by luminescent assay and observed no baseline differences (Fig 4B). To assess energetic status upon
195 challenge, we exposed worms to the complex I inhibitor rotenone. This acute (1-hour) challenge
196 decreased whole-body ATP levels of sugar-fed worms 40% more than controls (Fig 4B). To determine if
197 energetic responses in the CEP neurons follow the same trend as the whole-organism responses, and
198 assess whether that susceptibility would manifest in the context of the 6-OHDA challenge that we used
199 for neurodegeneration, we exposed worms expressing the PercevalHR ATP:ADP ratio reporter in
200 dopaminergic neurons to 50 mM 6-OHDA and vehicle controls of ascorbic acid. Surprisingly, ATP:ADP
201 ratio within the CEP neuron soma was not different across diets before or after 6-OHDA exposure (Fig
202 4C). Notably, ascorbic acid, the vehicle for 6-OHDA, induced significant ATP depletion. As ascorbic acid
203 does not induce neurodegeneration, and both sugars protected from neurodegeneration without

204 protecting from ATP depletion, our results are inconsistent with ATP depletion causing degeneration of
205 the CEP neurons.

206 **High sugar diets do not alter organismal antioxidant gene expression or alter glutathione**
207 **concentrations**

208 The third mechanism we tested for sugar-mediated dopaminergic neuroprotection was upregulation of
209 antioxidant defenses. Acute high sugar diets have been demonstrated to increase oxidative stress;
210 however, more chronic exposure in young adults increased expression of the proteins glucose-6-
211 phosphate 1-dehydrogenase and glutathione disulfide reductase, which should allow for accelerated
212 reduction of glutathione and confer protection from oxidant exposures (39). We hypothesized that
213 chronic high-sugar diets might cause similar compensatory and protective upregulation of antioxidant
214 systems, which could combat redox stress induced by 6-OHDA exposure. First, we assessed if our
215 chronic high sugar diets altered organismal redox state using a whole-animal reduction oxidation
216 sensitive GFP (roGFP) construct that reports on the ratio of oxidized to reduced glutathione. Due to the
217 increase in autofluorescence at 405nm driven primarily by gut autofluorescence (Supp Fig 2A-B), we
218 restricted our analysis to the head region from the tip of the head of the worm to the end of the
219 terminal pharyngeal bulb. High sugar diets induced no differences in the redox tone of the glutathione
220 pool on an organismal level (Fig 5A). To ensure that the lack of alteration in glutathione redox state was
221 not due to differences in total glutathione pool sizes, we quantified total glutathione levels and found no
222 statistically significant difference (Fig 5B). To determine if this result, which was contrary to findings
223 from acute exposures, was due to altered antioxidant gene expression, we evaluated the mRNA
224 expression levels of multiple antioxidant enzymes. Again, we observed no significant differences (Fig 5C,
225 SFig 4). Finally, to test the redox state specifically within the mitochondria of the CEP neurons that were
226 targeted by 6-OHDA in our neurodegeneration studies, we utilized a CEP neuron-specific mitochondrial-
227 targeted roGFP. In accordance with the organismal result, no difference was observed as a result of the

228 high sugar diets. However, sugar-fed worms had a significantly smaller increase in oxidation state after
229 6-OHDA exposure (Fig 5D). This result is consistent with protection from neurodegeneration and is
230 supportive of oxidative stress as a driver of neurodegeneration. However, it could be explained either by
231 a cell-specific increase in antioxidant defenses, not detectable by our whole-organism measurements, or
232 by a decrease in 6-OHDA uptake by the dopaminergic neurons. We next tested the latter possibility.

233 **High sugar diets modulate the dopamine transport system to decrease dopamine reuptake**

234 6-OHDA is actively transported into the dopaminergic neurons by the DAT-1 transporter. Each worm has
235 only 4 CEP neurons, which makes direct quantification of the uptake of 6-OHDA impractical. Therefore,
236 we instead we measured proxies for the quantity and activity of the DAT-1 transporter. We assessed
237 mRNA expression of *dat-1*, the re-uptake transporter responsible for 6-OHDA transport into the CEP
238 neurons; *cat-2*, which encodes tyrosine hydroxylase, the rate limiting step in dopamine synthesis; and
239 the dopamine receptor *dop-3* (Fig 6A). With no alterations in expression levels observed, we next
240 investigated the functional status of dopaminergic neurotransmission, using a swimming induced
241 paralysis (SWIP) assay. Release of dopamine into the neuro-muscular junction dictates the ability of the
242 muscle cells in worms to contract and relax. When too much dopamine enters the junction, or not
243 enough is cleared via re-uptake, the worms are temporarily paralyzed. After 10 minutes of swimming,
244 glucose and fructose fed worms were five and two times more likely to SWIP (Fig 6B). Increased SWIP
245 activity may indicate decreased dopamine reuptake by the CEP neurons, which would protect against 6-
246 OHDA uptake.

247 Discussion:

Table 1: Summary of previous research on high glucose and high fructose diets in *C. elegans*

Article	Sugar	Dose (mM)	Exposure paradigm	Lifespan	Brood Size	Oxidative Stress	Locomotion	Lipid Content	Neurodegeneration

Alcantar-Fernandez (2018)(15)	G	20, 40, 80, 100	L1-L4	↓26-52%	⊘ F0 ↓ F1, F2	↑	-	↑2-3 fold	-
Salim (2014)(17)	G	111	L1-L4	↓32%	↓30%	-	↓18%	-	↑
Garcia (2015)(19)	G	3.5-111	D1 adults to end of assay	↓ (anoxic conditions)	-	-	-	↑	-
	F	3.5-111	D1 adults to end of assay	↓ (anoxic conditions)	-	-	-	-	-
Schlotterer (2009)(40)	G	40	D1 adult to end of life	↓ 2 days	-	↑ D15 adults	-	-	-
Lodha (2020)(20)	F	277.5	L4 to end of life	↓ 5%	-	-	↓ 52% D10 adults	-	-
Tauffenberger (2014)(41)	G	277.5	L4 to end of life	↓F0 ⊘ F1 and F2	↓ F0, F1, F2	↓ F0 F1 (enhanced juglone survival)	-	-	↑ F0
Zhu (2015)(42)	G	100, 200	L1-L4	↓29.0% and 30.8%	-	↑	-	↑ (strain VS29)	-
Seung-Jae Lee (2009)(43)	G	111	D1 adult to end of life	↓ 20%	-	-	-	-	-
Liggett (2015)(44)	G	250	L4 to end of life	↓30-40% hermaphrodite ↑10% males	-	-	↓ 43% hermaphrodites, 7% males (D14)	-	-
Teshiba (2016)(45)	G	10, 50, 100	L4 to end of life	-	⊘ 100	-	-	-	-
Alcantar Fernandez (2019)(16)	G	20, 40, 80, 100	L1 to L4	-	-	↑ in all	-	-	-

Zheng (2017)(46)	G	111	L1 to end of life	↓	-	-	-	↑	-
	F	55, 111, 555	L1 to end of life	↑ at 55 and 111 ↓ at 555	-	-	-	⊘ at 55 and 111 ↑ at 555	-
Ke (2021)(47)	F	55.5	L4 to assay or end of life	↓	-	-	↓	↑ D1 adults	-
Gatrell (2020)(48)	G	250	L4 to assay or end of life	↓	⊘	-	↓	-	⊘ polyQ aggregation
Beaudoin-Chabot (2022)(49)	G	111	Adult D1 or D5 to end of life	↓ D1 ↑ D5	-	↑ D1 and D5, measured at D10	↓ D1 ↑ D5 Measured after 24-hour exposure	-	-
Engstrom (2022)(50)	G	333	Either only as L4 or adult, or both	-	↓ if fed glucose as adult ⊘ if only fed glucose as L4	-	-	-	-
Mondoux (2011)(51)	G	100, 200, 300, 400, 500	L4 to assay	-	↓at all but 200 ⊘ at 200	-	-	-	-
Xiong Wang (2020)(52)	G	5 50 400 500 520	L1 to end of life for lifespan L4 to end of life for brood size	↑ 14.36-27.55% from 5-500 ↓ 35.69% at 520	⊘ 5-50 ↓ 400-520	-	-	-	-
	F	5 50 400 500 550	L1 to end of life for lifespan L4 to end of life for brood size	↑ 1.52-23.36% from 5-400 ↓ 0.36-1.15% at 500-550	↑ from 5-50 ↓ 400-550	-	-	-	-

Gusarov (2019)(39)	G	111	L4 to assay	↓ 28%	-	⊘ at baseline ↓ as it protects from oxidants	-	↑ at D3 adult	-
This work	G	100	D1-D5 of adulthood	↓	↓	⊘ at baseline ↓ as it protects from 6-OHDA	↓	↑	⊘ at baseline ↓ as it protects from 6-OHDA
	F	100	D1-D5 of adulthood	↓	↓	⊘ at baseline ↓ as it protects from 6-OHDA	↓	↑	⊘ at baseline ↓ as it protects from 6-OHDA

Summary of previous and current work studying the impact of high glucose and high fructose diets in *C. elegans*. Sugar: glucose (G) or fructose (F); ↓ represents a decrease, ↑ represents an increase, and ⊘ represents no detected difference

Sugars such as glucose and fructose are essential for animal life, but diets containing excessive sugar can increase neurodegeneration in mammalian models and *C. elegans* (18, 23, 48, 53). We expand on previous investigations of high sugar diets in C. elegans to investigate mechanistic links between high sugar, mitochondrial disfunction, and dopaminergic neurodegeneration (Table 1). Our exposure paradigm begins in early adulthood, but like previous work still leads to decreased lifespan, increased lipid accumulation, and decreased reproduction. Despite these similarities, our results were inconsistent with previous findings in which high glucose induced degeneration of dopaminergic neurons, decreased dopamine levels, and exacerbated monocrotophos-induced neurotoxicity (18, 54). In this study we did not find a change in neurodegeneration after chronic, non-developmental high-glucose and high-fructose diets. Rather, we found that these diets protected from 6-OHDA-induced dopaminergic neurodegeneration. After assessing a number of potential mechanisms of protection, we propose that the protective effect is mediated by decreased 6-OHDA uptake via the DAT-1 transporter.

261 Counter to previous work showing electron transport chain impairment and severe
262 mitochondrial dysfunction (16, 20, 53), we only identified a slight elongation of the mitochondria in
263 dopaminergic neurons of glucose fed worms, and no change in those fed fructose. No difference in
264 mitochondrial function was detected with whole worm respirometry, total ATP levels, or ATP:ADP ratio
265 within the CEP neurons. The only apparent indication of bioenergetic dysfunction induced by the high
266 sugar paradigm was in response to challenge by the Complex I inhibitor rotenone, which caused nearly
267 40% greater ATP depletion in sugar-fed worms. 80 mM and 100 mM glucose dose-dependently
268 decreased the activity of Complex I in a previous *C. elegans* study, without alteration to ATP, ADP, or
269 AMP concentrations (16). It is plausible that lower Complex I activity decreased the dose of rotenone
270 required to completely inhibit Complex I function, or that glycolysis is already enhanced by the high
271 sugar diets, preventing further transition to glycolytic metabolism. We previously demonstrated the
272 upregulation of glycolysis in rotenone-treated worms (55) , though not in the context of high-sugar
273 diets. Because different cell types rely on different bioenergetic pathways, we next tested whether the
274 increased susceptibility to acute electron transport chain inhibition we observed on the organismal level
275 would also be observed within the CEP neurons. Remarkably, sugar-fed worms showed no discernable
276 difference in ATP:ADP ratio after 6-OHDA exposure, which is inconsistent with energetic deficit causing
277 neurodegeneration, since the same sugar exposures protected against 6-OHDA-induced
278 neurodegeneration. Furthermore, as the vehicle in our neurodegeneration experiments also decreases
279 ATP:ADP ratio but did not cause neurodegeneration, it is improbable ATP depletion is the mechanistic
280 step responsible for 6-OHDA induced dopaminergic neurodegeneration. Earlier work characterizing
281 rotenone similarly noted that redox stress, not ATP depletion, is critical for its induction of
282 neurodegeneration (56, 57).

283 Numerous studies with acute sugar exposure models have detected increased antioxidant
284 enzyme expression or increased total glutathione levels (15, 39), which would protect from the oxidative

285 stress induced by 6-OHDA. However, we found no differences in total glutathione, redox tone of the
286 glutathione pool, or expression of antioxidant enzymes in the glutathione-related, superoxide
287 dismutase, catalase, peroxiredoxin, or thioredoxin families. It is possible that differences in mRNA
288 and/or protein levels specifically within the CEP neurons existed but were not detected in our whole-
289 organism gene expression analysis. However, many previous studies that detected upregulated
290 antioxidant defenses after acute exposures also employed whole-organism measures, making this
291 explanation less likely. Our chronic exposure paradigm may result in adaptations across the lifetime of
292 the worm in glucose uptake, transport, and utilization culminating in a loss of the acute-phase oxidative
293 stress response, explaining our lack of effects. Despite finding a decreased oxidative response to 6-
294 OHDA in the CEP neurons of sugar-fed worms, it is unlikely a result of enhanced antioxidant defenses.
295 Having ruled out redox changes and bioenergetic inhibition as the mechanism for neuroprotection, we
296 next considered the possibility of altered 6-OHDA uptake in high-sugar fed worms.

297 The DAT-1 transporter is required for 6-OHDA uptake into the CEP neurons and inhibition of
298 DAT-1 is protective from 6-OHDA induced degeneration (31, 32). *dat*-1 mutants were among the
299 earliest to be identified as sensitized to swimming induced paralysis (SWIP), and synaptic localization of
300 DAT-1 is required for to prevent SWIP (58). Our account of the increased tendency towards SWIP after
301 sugar exposure is consistent with modified dopamine transport in these worms. This could be an
302 attempt to maintain dopamine in the synaptic cleft despite lower total dopamine levels, a possibility
303 bolstered by recent evidence that high glucose diets decrease dopamine levels (54). Though little work
304 has explored the relationship between DAT-1 and high sugar diets, recent work in *C. elegans*
305 demonstrated 80% decreased fluorescence of *dat-1* promoter driven GFP after high-glucose exposure
306 (54). In mammalian models, high glucose diets activate PKC, which drives DAT endocytosis, opening the
307 possibility for a similar high sugar driven effect in worms (59-61). Notably, alterations to SWIP were not
308 associated with increased neurodegeneration.

309 Beyond the toxicant-induced neurological impacts, we also deepen understanding of how the two most
310 consumed sugars compare in their biological effects. High-glucose and high-fructose diets in our study
311 produced similar but non-identical effects in nearly all experiments. Only glucose-fed worms exhibited
312 elongated neuronal mitochondria, and in general, apart from lifespan, fructose-fed worms typically
313 showed a less significant departure from controls than glucose-fed worms. These discrepancies may be
314 explained by differences in the metabolism of these sugars, but it remains clear that the pathways
315 driving alterations in dopaminergic function, lifespan, reproduction, and ATP production are impacted in
316 very similar ways. This may indicate that in models with more complex organ systems, where stronger
317 differences between sugar types have been observed, those differences are driven by tissue-specific
318 metabolism and responses. For example, fructokinase, fructose bisphosphate aldolase-B, and
319 dihydroxyacetone kinase, the three enzymes responsible for fructose metabolism, are only found in the
320 liver and kidney of rats (62). In *C. elegans*, hexokinases (HXK-1,2,3) predicted to be the first step in
321 fructose metabolism, are expressed ubiquitously (63). Thus, the reported mitochondrial swelling and
322 respiratory dysfunction induced only by fructose in rat livers may be a result of specific mitochondrial
323 dynamics and concentrated fructose metabolites in the liver and kidneys, versus the potentially non-
324 tissue-specific metabolism in worms (64). It should be noted, in the same study in rats, high sugar diets
325 had generally similar effects on fatty acid oxidation and mitochondrial protein acetylation in isolation,
326 but divergent effects when supplemented on top of a high fat diet (64). Thus, further examination of
327 dietary components in isolation and combination will be required to understand the complex dynamics
328 governing effects of different sugars and how they relate to other model organisms.

329 The interaction between diet and toxicant exposure remains an active area of investigation due
330 to the plethora of dietary alterations and chemicals (65-70). High sugar diets elucidate several metabolic
331 and oxidative stress pathway alterations, depending on the exposure paradigm, leading to interactions
332 with toxicants that target the same pathways. In *Drosophila melanogaster*, high glucose enhances

333 Bisphenol A toxicity by exacerbating downregulation of testis-specific genes and upregulation of
334 ribosome-associated genes (70). In *C. elegans*, high sugar diets increase susceptibility to monocrotophos
335 and parathion, including increasing the damage inflicted on dopaminergic neurons (17, 18, 71). We
336 show that both high-glucose and high-fructose decrease susceptibility to 6-OHDA induced
337 neurodegeneration but enhance susceptibility to rotenone induced ATP depletion. Together, these data
338 highlight the critical need to continue assessing toxicant by diet interactions for multiple endpoints, as
339 the outcomes are likely highly specific to the tissue of interest and toxicokinetics of each chemical used.

340 There are also limitations to our study. We do not address how ecologically relevant
341 neurotoxicants would interact with high sugar consumption. Due to the unique toxicokinetic effect of
342 DAT-1 on 6-OHDA uptake, which would not generally be conserved for other dopaminergic toxicants,
343 impacts of high sugar should be examined not only with ecologically relevant pollutants, but toxicants
344 with varied mechanisms of toxicity. It is also possible the mechanisms we observe are limited to our
345 exposure paradigm. As shown in Table 1, previous investigations often rely on developmental acute
346 exposures and show different neurodegenerative results. Further work is required to understand the
347 patterns of redox, bioenergetic, and dopaminergic transmission changes that occur both as a function of
348 age and sugar consumption.

349 Conclusions:

350 Non-developmental high-glucose and high-fructose diets are protective against 6-OHDA induced
351 dopaminergic neurodegeneration, potentially due to their modifications of dopamine transmission
352 processes decreasing 6-OHDA uptake. Intriguingly, this protection occurs despite decreased lifespan,
353 decreased fecundity, and increased lipid storage. As demonstrated by the lack of neurodegeneration
354 induced by ATP depletion, the induction of oxidative stress appears to be more important in the
355 induction of dopaminergic neurodegeneration by 6-OHDA. This study highlights the important

356 interactions between lifestyle factors such as diet, oxidative stress, and susceptibility to toxicant induced

357 dopaminergic neurodegeneration.

358

359

360 Materials and Methods:

361 Strains and Culture

362 The wild-type CGC (N2), LIU2, BY200, JMN080(pdat-1::MLS::GFP), SJ4103, JV2, PE255 (*feIs5*), and
363 PHX2923 (pdat-1::PercevalHR), PHX2867 (pdat-1::MLS::roGFP), were maintained at 20 C on K-agar plates
364 seeded with OP50 *E. coli*. For experiments, worms were synchronized through egg-lays as in which
365 worms were transferred onto new plates, allowed to lay eggs for 3 hours, then washed to remove
366 adults. They were aged to adulthood on K-agar plates seeded with OP50 *E. coli*. As D1 adults (72 hours
367 post egg lay), worms were evenly split between NGM, NGM + 100 mM glucose, or NGM + 100 mM
368 fructose plates freshly seeded with OP50 E. coli. They were transferred daily to freshly seeded plates to
369 discount effects of plate acidification. All worms were reared from D1-D5 of adulthood on their
370 respective group plate (control, glucose, or fructose). On D8 assays were run, initiated, or worms were
371 returned to K-agar OP50 plates as described for individual assays.

372 Generation of transgenic strains

373 *Generation of dat-1p::MLS::GFP*

374 To generate the *dat-1*p::MLS::GFP plasmid, a 886 bp fragment directly upstream of the dat-1 start codon
375 was amplified from wildtype (N2 Bristol type) genomic DNA, using primers with overhangs that
376 contained homology to a plasmid containing a mitochondrial localization sequence (MLS) and GFP,
377 Forward Primer 5'→3': agggcgaattgggtaccCGTCTCATTCCTCATCTCCGAGC and Reverse Primer: 5'→3':
378 GTGCCATatcgatGGCTAAAAATTGTTGAGATTCGAGTAAACCG. The mitochondrial localization sequence was
379 originally amplified from Fire Vector pPD96.32. pPD96.32 was a gift from Andrew Fire (Addgene plasmid
380 # 1504 ; http://n2t.net/addgene:1504 ; RRID:Addgene_1504). The amplified dat-1 promoter was
381 inserted into the plasmid containing the MLS and GFP using Gibson Assembly and insertion was
382 confirmed by colony PCR with a nested GFP reverse primer and M13 Forward primer. The plasmid was
383 sequenced to check for any mutations and co-injected with 50 ng/µl unc-119 rescue DNA, 50 ng/µl
384 pBsSK, and 50 ng/µl EcoR1 cut salmon sperm DNA into unc-119(ed4) hermaphrodites. Once
385 extrachromosomal lines were established and dat-1p::MLS::GFP signal was observed, plasmid was
386 integrated by gamma irradiation as previously described (72). Integrated lines were outcrossed with N2
387 to remove possible background mutations.

388 *Generation of dopaminergic neuron PercevalHR and mitochondrial roGFP*

389 Worm strains expressing mitochondrial targeted reduction oxidation sensitive GFP (roGFP) and
390 PercevalHR within the dopaminergic neurons were generated by SunyBiotech
391 (https://www.sunybiotech.com). Both constructs were cloned into the pPD95.77 vector and included
392 890 bp of the *dat-1* promoter (ending just upstream of the start codon) amplified from genomic DNA

393 and the 5'UTR from the *unc-54* gene present in the pPD95.77 vector. We inserted the reporter genes
394 immediately downstream of the *dat-1* promoter and upstream of the *unc-54* 5'UTR. The mito-roGFP2-
395 Grx1 coding sequence was adapted from pUAST mito roGFP2-Grx1 (Addgene Plasmid# 64995) by codon
396 optimizing for expression in *C. elegans* using the *C. elegans* Codon Adapter (73) and a single intron was
397 added 402 bp downstream of the start codon. The Perceval-HR coding sequence was adapted from
398 pRsetB-his7-Perceval (Addgene Plasmid# 20336) by codon optimizing for *C. elegans* expression and a
399 single intron was added 444 bp downstream from the start codon. The construction of the plasmids,
400 verification by sequencing, microinjection into animals, integration, and isolation of individual strains
401 were performed by SUNY Biotech. We received three low-copy-number strains for each construct, and
402 all three strains were phenotypically normal.

403

404 Fluorescence Microscopy

405 Strain and specific image analysis details are listed below for each individual endpoint. However, all
406 strains were imaged with a Keyence BZX-2710 microscope. Unless otherwise specified, worms were
407 transferred by stainless steel pick to 2% w/v agarose pads, anesthetized with 15-20 uL 0.5 M sodium
408 azide, and imaged immediately. All quantitative image analysis was performed using Fiji ImageJ
409 software. Background subtraction was performed for all quantitative microscopy by subtracting the
410 equivalent measurement (mean grey value, etc) of a region in the image without a worm present.

411 Fat Quantification

412 After 5 days of dietary exposure, LIU2 worms were washed off plates and washed three times with K-
413 medium to remove bacterial debris. Worms were visualized in brightfield and under and EGFP or
414 TexasRed filter with a 10X objective. Three independent experiments were conducted, with
415 approximately 20 worms per treatment group imaged in each. Worm bodies were outlined as the region
416 of interest (ROI) and mean grey value was determined within the full body of the worm.

417 Lifespan

418 Lifespan assays were carried out with few modifications from previous descriptions (source). After 5
419 days of dietary exposure, 50 BY200 transgenic worms from each treatment group were transferred to 6
420 cm K-agar plates seeded with OP50. Worms were transferred to fresh plates every third to fourth day
421 and monitored daily for death. Worms were considered dead if they displayed no touch response when
422 poked with a steel pick and no bodily movement was observed. Animals that crawled off the plate or
423 died due to vulval protrusion or bagging were censored. The data is represented as starting on day 8 as
424 only worms that were alive on day 8 were used for subsequent analysis.

425 Reproduction

426 Single worms were transferred to individual 6 cm NGM or NGM + sugar plates as late L4. They were
427 transferred to a second plate 48 hours later, then were transferred every 24 hours to the remaining
428 plates. Progeny were counted 48 hours after the adult was removed. At least 5 worms per treatment
429 were utilized in each of three biological replicates.

430 Dopaminergic Neurodegeneration

431 *Exposure and Imaging*
432 On day 5 of dietary exposure, worms were washed and dosed with 25 mM or 50 mM 6-
433 hydroxydopamine (6-OHDA) in 10 mM or 20mM Ascorbic Acid (AA) solution [Ascorbic Acid, K+ mixture
434 (K-medium, Cholesterol, $CaCl_2$, $MgSO_4$)]. Control groups were incubated in an identical volume of only
435 the AA solution. All groups were incubated for 1 hour with rocking and subsequently washed with K-
436 medium solution three times to ensure complete removal of 6-OHDA. They were replated on K-agar
437 plates seeded with 2X OP50 and incubated at 20 C for 48 hours prior to imaging. Images were obtained
438 with the 40X objective in Z-stacks encompassing the full head of the worm. Images were processed by
439 generating maximal value Z-projections of stacks with FIJI ImageJ software and cropped to only display
440 the head region of a single worm per image.
441
442 *Scoring*
443 Images were blindly scored with the open access software Blinder, by Solibyte solutions (74). Each
444 dendrite of the four CEP neurons of each worm were scored on a scale of 0-4, as follows:
445 0- no visible damage or abnormalities
446 1-blebs or kinks encompassing less than 50% of the dendrite
447 2-blebs or kinks on encompassing more than 50% of the dendrite
448 3-breaks present with more than 50% of the dendrite remaining
449 4-breaks present with less than 50% of the dendrite remaining
450 To ensure scoring validity, the built-in Quality Control feature was utilized, and images were rescored
451 until the error was less than 15%.
452

453 Seahorse Analysis

454 On day 5 of dietary exposure, whole worm respirometry was performed with a Seahorse Xf^e24
455 Extracellular flux analyzer as previously described (75), with the following modifications: Worms were
456 diluted to approximately 30 worms per well to maintain optimal oxygenation of the well during the
457 protocol and 40 uM DCCD was utilized to obtain maximal inhibition of mitochondrial electron transport
458 chain Complex V. 100-500 worms were reserved from each replicate and immediately imaged on K-agar
459 plates for size determination. Worm volume was quantified using the WormSizer ImageJ plugin for
460 normalization to worm volume .

461 Mitochondrial Morphology

462 On Day 5 of adulthood, strains SJ4103 and JMN080 worms were imaged with the 60X and 40X objectives
463 respectively. Images were taken as z-stacks encompassing the full muscle cell and maximally projected
464 for analysis in ImageJ. CEP neuron mitochondria were analyzed for the number and length of each
465 mitochondrion within each dendrite by using the line tool to manually trace each mitochondrion. Body
466 wall muscle mitochondria were analyzed for mean grey value per muscle cell as a proxy for total
467 mitochondrial mass.

468 Swimming Induced Paralysis

469 On day 5 of the dietary exposure protocol approximately 10 worms were picked by flame sterilized steel
470 pick into 100 uL of Millipore water in one well of a 96 well plate, each well was recorded for a minimum
471 of 10 minutes from the time the pick was removed from the water. Videos were analyzed for the
472 percentage of worms paralyzed at one-minute intervals for ten minutes, starting from the time the pick

473 entered the water. Worms were considered paralyzed when they were completely rigid for 5 second
474 intervals before and after the one-minute mark.

475 Autofluorescence

476 On day 5 of dietary exposure, Bristol N2 worms were imaged with the 10X objective under brightfield,
477 405 nm, and 488 nm excitation. The brightfield image was used to select the entire body of the worm as
478 the ROI and fluorescence was quantified in each respective channel as mean grey value.

479 roGFP and PercevalHR imaging

480 On day 5 of dietary exposure, dat-1p::MLS::roGFP or JV2 worms, were paralyzed with 1 mM levamisole
481 HCl and imaged. PercevalHR was mounted on 5% w/v agarose pads and imaged without paralytics. JV2
482 was imaged with the 10X objective and both dopaminergic strains were imaged with the 40X objective
483 at 405 nm and 488 nm excitation. Mean grey value was quantified and compared in as a ratio or
484 405/488 for roGFPs and 488/405 for PercevalHR.

485 qPCR

486 On day 5 of dietary exposure RNA was extracted via the Qiagen RNeasy Mini Kit (Qiagen 74104). Briefly,
487 100-200 worms were collected into conical tubes in K-medium. All animals were shaken for 10 minutes
488 on an orbital shaker to clear gut bacteria, transferred to a 1.5 mL microcentrifuge tube, and suspended
489 in RLT buffer. Samples were immediately flash frozen in liquid nitrogen and thawed on ice. Disruption of
490 the worm cuticle was then completed by bead beating with zirconia beads for 8 cycles of 30 seconds
491 beating and 1 minute on ice. Homogenate was then utilized in accordance with kit instructions. cDNA
492 was synthesized from 2 ug total RNA with a high-capacity cDNA Reverse Transcription Kit in 20 uL
493 reactions (Thermo Fischer, Ref. 4368814). We carried out qPCR using diluted cDNA, Power SYBR Greeen
494 Master Mix (Thermo Fischer 4368702) and 0.5 µM of gene-specific primers (Sup Table 1) in a CFX96
495 qPCR Real-Time PCR module with C1000 Touch Thermal Cycler (BioRad). After 10 minutes at 95°C, a
496 two-step cycling protocol was used (15 seconds at 95°C, 60 seconds at 60°C) for 40 cycles. We calculated
497 relative expression using the ΔΔCt method with cdc-42 and tba-1 as reference genes. Genes only
498 expressed in the dopaminergic neurons, dat-1, dop-3, and cat-2, required an additional 10 cycles of PCR
499 amplification prior to qPCR for adequate detection.

500 Total GSH levels

501 On day 5 of dietary exposure, 200 worms from each group were suspended in 75 uL of MES buffer in 1.7
502 mL conical tubes. Approximately 50 uL 0.5 mm zirconium oxide beads were added to each tube. Samples
503 were homogenized via bead beating (8 cycles, 30s on sonication, 30s without sonication at 4 C). Next, 65
504 uL of homogenate was recovered, with 10 uL transferred to a new tube for protein quantification and 55
505 uL diluted by half with 5% w/v metaphosphoric acid for total GSH quantification. GSH quantification was
506 completed in accordance with instructions for tissue homogenate (Cayman Chemical Kit No.703002).
507 Protein quantification for each sample was conducted by BCA Assay in accordance with kit instructions
508 (Millipore Sigma 71285M).

509 Whole Worm ATP Levels

510 Strain PE255 worms were reared in accordance with the dietary exposure protocol, challenged with 20
511 uM rotenone for 1 hour, and transferred to 96-well plates for Luciferin-based ATP quantification as

512 previously described (76). Luminescence was normalized to number of worms per well rather than GFP
513 due to autofluorescence differences.

514 Graphing and Statistical Analysis

515 GraphPad Prism version 9.5.0 was used for all graph generation and statistical testing. Statistical tests
516 are identified in the figure legend of each graph.

517

518

519

520

521 Figure Legends:

522 Figure 1. High-sugar diets increase lipid content, decrease reproduction, and shorten lifespan. **A** Fat
523 quantification and **B** representative images of 8-day old LIU2 worms reared on control (n=77),100 mM
524 glucose (n=83), or 100 mM fructose (n=74) supplemented NGM plates with OP50 as a food source. **C**
525 Total number of progeny (n=15 per treatment) **D** progeny laid per day (n=15, per treatment, p-
526 interaction<0.0001) of individual worms plated on 6 cm control or sugar supplemented plates from late
527 L4 to post-reproductive age. **E** Lifespan analysis of worms treated from days 1-5 of adulthood on control
528 (n=141, median survival 23 days), glucose (n=146, median survival 21 days, p=0.0271), or fructose
529 (n=137, median survival 17 days, p=0.0001) supplemented NGM plates then transferred to K-agar OP50
530 plates until death. Only worms that were alive on day 5 of adulthood were utilized. For **A-D**, Shapiro
531 Wilks normality tests were used to confirm distribution normality of the data. One-way ANOVA followed
532 by Tukey's Post-Hoc was used for A and C to determine p-value. For D, a two-way ANOVA with Tukey's
533 post-hoc was used. For **E**, a Kaplan-Meier survival analysis was performed in conjunction with the Log-
534 rank test. *p<0.0332, **p<0.0021, ***p<0.0002, ****p<0.0001

535 Figure 2. High-sugar diets do not induce neurodegeneration and protect from the neurotoxicant 6-
536 hydroxydopamine (6-OHDA). **A** Representative images for each of the 5 scores used to assess
537 dopaminergic neurodegeneration **B** A comparison of neurodegeneration in control, glucose-fed, and
538 fructose-fed worms treated with a vehicle control of 5 mM Ascorbic Acid or 25 mM or 50mM of 6-
539 OHDA. Pairwise chi-squared analysis was run with a Bonferroni corrected p-value of < 0.003571 to
540 account for 14 pairwise comparisons.

541 Figure 3. High-glucose diet induces mild neuronal mitochondrial elongation. **A** The number of
542 mitochondria per dendrite, **B** average length of mitochondria per dendrite, **C** length of the longest
543 mitochondria per dendrite, and **D** sum of the lengths of all mitochondria within a dendrite in worms
544 reared on control (n=249), 100 mM glucose (n=127), or 100 mM fructose (n=134) supplemented NGM
545 plates. **A-D** Shapiro-Wilks Normality tests determined all data sets were non-normally distributed.
546 Kruskal-Wallis test followed by Dunn's multiple comparisons was used to establish p-values for
547 comparisons. *p<0.0332, **p<0.0021, ***p<0.0002, ****p<0.0001

548 Figure 4. High sugar diets do not alter baseline bioenergetics or protect from ATP depletion from
549 mitochondrial inhibitors. **A** Whole worm respirometry was performed on D8 worms after high-sugar diet

550 exposure to quantify mitochondrial respiratory function. Oxygen consumption rate was normalized to
551 worm number and volume to account for differences in body size. **B** Whole worm ATP levels were
552 quantified after dietary exposure to either control, high-glucose, or high-fructose conditions. Control,
553 glucose, and fructose exposed worms were also subjected to a 1-hour 20 uM rotenone challenge to
554 assess organismal response to electron transport chain inhibition. **C** Worms expression dat-
555 1::PercevalHR were exposed to control, high-glucose, or high-fructose conditions, and assessed on day 8
556 under after exposure to ascorbic acid or 50 mM 6-OHDA. *p<0.0332, **p<0.0021, ***p<0.0002,
557 ****p<0.0001

558 Figure 5. High-sugar diets protect from 6-OHDA induced oxidative stress without detectable alteration to
559 antioxidant systems. **A** The redox tone of the glutathione pool was quantified to assess organismal
560 oxidative stress. Worms expressing roGFP ***** were reared from day 1-5 of adulthood on NGM plates
561 or NGM supplemented with 100 mM glucose or fructose. Control worms were exposed to 3% H2O2 as a
562 positive control for increased oxidation. **B** Subsequently, organismal total glutathione levels were
563 assessed control, glucose, and fructose fed worms. **C** Alterations to mRNA levels of multiple families of
564 antioxidants were assessed for alterations by qPCR. **D** To examine redox response within the CEP
565 neurons to 6-OHDA, worms expressing *dat-1*::mls roGFP were used and exposed to control, vehicle (5
566 mM Ascorbic Acid) or 50 mM 5-OHDA on day 5 of adulthood. **A-B** Normality was confirmed by a
567 Shapiro-Wilks normality test; One-way ANOVA followed by Tukey's Post-hoc was used to determine p-
568 values. **C** Relative gene expression was determined by the ΔΔCt method, and each gene was analyzed by
569 one-way ANOVA with Tukey's Post-hoc. **D** One-way ANOVA followed by Tukey's Post-hoc was used to
570 determine p-values. For all panels *p<0.0332, **p<0.0021, ***p<0.0002, ****p<0.0001

571 Figure 6. Dopamine transmission is altered in sugar-fed animals. **A** Relative expression of dopamine
572 synthesis, reuptake, and transporter genes was assessed via qPCR in worms reared on control NGM or
573 high-glucose or high-fructose supplemented plates. A one-way ANOVA with Tukey's post hoc was used
574 to determine p-values. **B** The tendency of sugar fed worms to undergo swimming induced paralysis
575 (SWIP) was determined. A two-way ANOVA with Dunn's post hoc was used to assess significance.
576 *p<0.0332

577

578 Supplementary Figure 1. Muscle cell mitochondrial mean grey value. SJ4103 worms were reared in
579 accordance with the dietary exposure protocol and imaged on day 8. Images were obtained using a
580 Keyence BZ-X710 with 60X magnification (oil immersion). Z-stacks were set to encompass the entirety of
581 the cell, and maximum projected for analysis. Individual cells were outlined as the region of interest for
582 analysis in Image J. Mean grey value was used as a proxy for total mitochondrial area (One-way ANOVA).

583 Supplementary Figure 2. Oxygen consumption rate normalized to worm number without accounting for
584 worm size. Whole worm respirometry was performed with the Seahorse XF24 Bioanalyzer and reported
585 as oxygen consumption rate normalized to the number of worms in each well. All wells from the same
586 biological replicate were averaged to produce n=1 (One-way ANOVA, Tukey's Post Hoc, *p<0.0332).

587 Supplementary Figure 3. Autofluorescence quantification at 488 nm and 405 nm excitation wavelengths.
588 N2 (wild-type) worms were reared on their respective sugar diets and imaged at day 5 of adulthood to
589 determine if high sugar diets alter worm autofluorescence. No significant difference was detected in the

590 N2 strain at 488 nm, however both high glucose and high fructose diets increase autofluorescence at
591 405 nm excitation (One way ANOVA, Tukey's Post Hoc,**p<0.0021,****p<0.0001)

592

593 Supplementary Table 1. Primers utilized for RT-qPCR

Gene	Forward (5'-3')	Reverse (5'-3')
cat-2	GGCGTTAGAGTTCAAGTTTGGT	CCGCTGTCAAAACCTTCTCC
cdc-42	GAGAAAAATGGGTGCCTGAA	CTCGAGCATTCCTGGATCAT
ctl-1,2,3	ACTAAAGTTTGGCCACACGG	CTTGGAGCATCTTGTCTGGC
dat-1	TTTTGCCATCCGGGTAGAGTC	GACATTGCTCTTTCCCTCTTCG
dop-3	CTTCTTGCTCGCTCTCGTTG	TGGAAGAGAACGATGAATGCG
gcs-1	ACAAGCCGAAGAGCAGGTGAATG	GCAAGCGATGAGACCTCCGTAAG
gsr-1	CGGATTTGATGTGACGCTTA	AAAGTTGCACGTCCTCGAAT
gst-1	CCGTCATCTCGCTCGTCTTAATGG	AGCCTTGCCGTCTTCGTAGTTTC
gst-10	TGGGAAGAGTTCATGGCTTG	AACTTCACTAGAGCCTCCGG
gst-4	AGTTGTTGAACCAGCCCGTGATG	GCCCAAGTCAATGAGTCTCCAACG
prdx-2	TATCGCCTTCTCTGACCGTG	AAGAGTCCACGGAAAGCAATT
sod-1	AAAATGTCGAACCGTGCTGT	CCGGGAGTAAGTCCCTTGAT
sod-2	CTCGCTGCCAGATTTACCAT	TGAACTTGAGAGCTGGCTGA
sod-3	GCAATCTACTGCTCGCACTG	CAGCCTCGTGAAGTTTCTCC
sod-5	AAACGTGCTGTAGCGGTTCT	TCCATGAAGTCCTGGTGACA
trx-1	AGCGGAAGATCTTTGTTCCA	AATTGCGTCTCCATTCTTGG
tba-1	TCATCTCGCAGGTTGTGTCT	GGTAAGCCTTGTCAGCAGAG

594

595 Availability of Data and Materials: *C. elegans* strains JMN080, PHX2923, and PHX2867 are available from
596 the corresponding author upon request. All other strains are available from the *C. elegans* Genome
597 Center. All data and the source video and images are available upon request.

598

599

600 Acknowledgements: This work was funded by NIH awards K99-ES029552 (JHH), NIEHS P42ES010356
601 (JNM), NIEHS T32ES021432 (KSM), and R01ES034270 (JNM), and strains were provided by the
602 Caenorhabditis Genetics Consortium.

603

604 References:

605 1. USDA Sugar Supply: Tables 51-53; US Consumption of Caloric Sweeteners. In: Service USDoAER,
606 editor. 2012.
607 2. Safety WHONaF. Guideline: Sugar Intake for Adults and Children In: Safety NaF, editor.: World
608 Health Organization 2015. p. 49.

3. Johnston RD, Stephenson MC, Crossland H, Cordon SM, Palcidi E, Cox EF, et al. No Difference Between High-Fructose and High-Glucose Diets on Liver Triacylglycerol or Biochemistry in Healthy Overweight Men. Gastroenterology. 2013;145(5):1016-25.e2.
4. Malik VS, Schulze MB, Hu FB. Intake of sugar-sweetened beverages and weight gain: a systematic review. Am J Clin Nutr. 2006;84(2):274-88.
5. Hruby A, Hu FB. The Epidemiology of Obesity: A Big Picture. Pharmacoeconomics. 2015;33(7):673-89.
6. Health Effects of Overweight and Obesity in 195 Countries over 25 Years. New England Journal of Medicine. 2017;377(1):13-27.
7. Palavra NC, Lubomski M, Flood VM, Davis RL, Sue CM. Increased Added Sugar Consumption Is Common in Parkinson's Disease. Front Nutr. 2021;8.
8. Haas J, Berg D, Bosy-Westphal A, Schaeffer E. Parkinson’s Disease and Sugar Intake—Reasons for and Consequences of a Still Unclear Craving. Nutrients. 2022;14(15):3240.
9. Raza C, Anjum R, Shakeel NuA. Parkinson's disease: Mechanisms, translational models and management strategies. Life Sciences. 2019;226:77-90.
10. Santiago JA, Potashkin JA. Blood Biomarkers Associated with Cognitive Decline in Early Stage and Drug-Naive Parkinson’s Disease Patients. PLOS ONE. 2015;10(11):e0142582.
11. Mollenhauer B, Zimmermann J, Sixel-Döring F, Focke NK, Wicke T, Ebentheuer J, et al. Baseline predictors for progression 4 years after Parkinson's disease diagnosis in the De Novo Parkinson Cohort (DeNoPa). Mov Disord. 2019;34(1):67-77.
12. Palavra NC, Lubomski M, Flood VM, Davis RL, Sue CM. Increased Added Sugar Consumption Is Common in Parkinson's Disease. Front Nutr. 2021;8:628845-.
13. Sánchez-Gómez A, Alcarraz-Vizán G, Fernández M, Fernández-Santiago R, Ezquerra M, Cámara A, et al. Peripheral insulin and amylin levels in Parkinson's disease. Parkinsonism & Related Disorders. 2020;79:91-6.
14. Mondoux MA, Love DC, Ghosh SK, Fukushige T, Bond M, Weerasinghe GR, et al. O-Linked-N-Acetylglucosamine Cycling and Insulin Signaling Are Required for the Glucose Stress Response in Caenorhabditis elegans. Genetics. 2011;188(2):369-82.
15. Alcántar-Fernández J, Navarro RE, Salazar-Martínez AM, Pérez-Andrade ME, Miranda-Ríos J. Caenorhabditis elegans respond to high-glucose diets through a network of stress-responsive transcription factors. PLOS ONE. 2018;13(7):e0199888.
16. Alcántar-Fernández J, González-Maciel A, Reynoso-Robles R, Pérez Andrade ME, Hernández-Vázquez AdJ, Velázquez-Arellano A, et al. High-glucose diets induce mitochondrial dysfunction in Caenorhabditis elegans. PLOS ONE. 2019;14(12):e0226652.
17. Salim C, Rajini PS. Glucose feeding during development aggravates the toxicity of the organophosphorus insecticide Monocrotophos in the nematode, Caenorhabditis elegans. Physiology & Behavior. 2014;131:142-8.
18. Salim C, Rajini PS. Glucose-rich diet aggravates monocrotophos-induced dopaminergic neuronal dysfunction in Caenorhabditis elegans. Journal of Applied Toxicology. 2017;37(6):772-80.
19. Garcia AM, Ladage ML, Dumesnil DR, Zaman K, Shulaev V, Azad RK, et al. Glucose Induces Sensitivity to Oxygen Deprivation and Modulates Insulin/IGF-1 Signaling and Lipid Biosynthesis in Caenorhabditis elegans. Genetics. 2015;200(1):167-84.
20. Lodha D, Rajasekaran S, Jayavelu T, Subramaniam JR. Detrimental effects of fructose on mitochondria in mouse motor neurons and on C. elegans healthspan. Nutritional Neuroscience. 2020:1-10.
21. Cooper JF, Van Raamsdonk JM. Modeling Parkinson's Disease in C. elegans. J Parkinsons Dis. 2018;8(1):17-32.

656 22. Caldwell KA, Willicott CW, Caldwell GA. Modeling neurodegeneration in Caenorhabditiselegans.
657 Dis Model Mech. 2020;13(10).
658 23. Pinkas A, Lawes M, Aschner M. System-specific neurodegeneration following glucotoxicity in the
659 C. elegans model. NeuroToxicology. 2018;68:88-90.
660 24. Li Y, Chen Q, Liu Y, Bi L, Jin L, Xu K, et al. High glucose-induced ROS-accumulation in embryo-
661 larval stages of zebrafish leads to mitochondria-mediated apoptosis. Apoptosis. 2022;27(7):509-20.
662 25. Barouki R, Gluckman PD, Grandjean P, Hanson M, Heindel JJ. Developmental origins of non-
663 communicable disease: Implications for research and public health. Environmental Health.
664 2012;11(1):42.
665 26. Grandjean P, Barouki R, Bellinger DC, Casteleyn L, Chadwick LH, Cordier S, et al. Life-Long
666 Implications of Developmental Exposure to Environmental Stressors: New Perspectives. Endocrinology.
667 2015;156(10):3408-15.
668 27. Hershberger KA, Rooney JP, Turner EA, Donoghue LJ, Bodhicharla R, Maurer LL, et al. Early-life
669 mitochondrial DNA damage results in lifelong deficits in energy production mediated by redox signaling
670 in Caenorhabditis elegans. Redox Biology. 2021;43:102000.
671 28. Mello DF, Bergemann CM, Fisher K, Chitrakar R, Bijwadia SR, Wang Y, et al. Rotenone Modulates
672 Caenorhabditis elegans Immunometabolism and Pathogen Susceptibility. Front Immunol.
673 2022;13:840272.
674 29. Schober A. Classic toxin-induced animal models of Parkinson's disease: 6-OHDA and MPTP. Cell
675 and Tissue Research. 2004;318(1):215-24.
676 30. Bijwadia SR, Morton KS, Meyer JN. Quantifying Levels of Dopaminergic Neuron Morphological
677 Alteration and Degeneration in Caenorhabditis elegans. JoVE.e62894.
678 31. Masoudi N, Ibanez-Cruceyra P, Offenburger S-L, Holmes A, Gartner A. Tetraspanin (TSP-17)
679 Protects Dopaminergic Neurons against 6-OHDA-Induced Neurodegeneration in C. elegans. PLOS
680 Genetics. 2014;10(12):e1004767.
681 32. Nass R, Hall DH, Miller DM, Blakely RD. Neurotoxin-induced degeneration of dopamine neurons
682 in Caenorhabditis elegans. Proceedings of the National Academy of Sciences. 2002;99(5):3264-9.
683 33. Yu T, Robotham JL, Yoon Y. Increased production of reactive oxygen species in hyperglycemic
684 conditions requires dynamic change of mitochondrial morphology. Proceedings of the National Academy
685 of Sciences. 2006;103(8):2653-8.
686 34. Youle RJ, van der Bliek AM. Mitochondrial Fission, Fusion, and Stress. Science.
687 2012;337(6098):1062-5.
688 35. Meyer JN, Leuthner TC, Luz AL. Mitochondrial fusion, fission, and mitochondrial toxicity.
689 Toxicology. 2017;391:42-53.
690 36. Yu T, Sheu S-S, Robotham JL, Yoon Y. Mitochondrial fission mediates high glucose-induced cell
691 death through elevated production of reactive oxygen species. Cardiovascular Research. 2008;79(2):341-
692 51.
693 37. Jadiya P, Garbincius JF, Elrod JW. Reappraisal of metabolic dysfunction in neurodegeneration:
694 Focus on mitochondrial function and calcium signaling. Acta Neuropathologica Communications.
695 2021;9(1):124.
696 38. Pathak D, Shields LY, Mendelsohn BA, Haddad D, Lin W, Gerencser AA, et al. The Role of
697 Mitochondrially Derived ATP in Synaptic Vesicle Recycling *[♦]. Journal of Biological
698 Chemistry. 2015;290(37):22325-36.
699 39. Gusarov I, Pani B, Gautier L, Smolentseva O, Eremina S, Shamovsky I, et al. Glycogen controls
700 Caenorhabditis elegans lifespan and resistance to oxidative stress. Nat Commun. 2017;8:15868.
701 40. Schlotterer A, Kukudov G, Bozorgmehr F, Hutter H, Du X, Oikonomou D, et al. C. elegans as
702 Model for the Study of High Glucose– Mediated Life Span Reduction. Diabetes. 2009;58(11):2450-6.

703 41. Tauffenberger A, Parker JA. Heritable Transmission of Stress Resistance by High Dietary Glucose
704 in Caenorhabditis elegans. PLOS Genetics. 2014;10(5):e1004346.
705 42. Zhu G, Yin F, Wang L, Wei W, Jiang L, Qin J. Modeling type 2 diabetes-like hyperglycemia in C.
706 elegans on a microdevice. Integr Biol (Camb). 2016;8(1):30-8.
707 43. Lee S-J, Murphy CT, Kenyon C. Glucose Shortens the Life Span of C. elegans by Downregulating
708 DAF-16/FOXO Activity and Aquaporin Gene Expression. Cell Metabolism. 2009;10(5):379-91.
709 44. Liggett MR, Hoy MJ, Mastroianni M, Mondoux MA. High-glucose diets have sex-specific effects
710 on aging in C. elegans: toxic to hermaphrodites but beneficial to males. Aging (Albany NY).
711 2015;7(6):383-8.
712 45. Teshiba E, Miyahara K, Takeya H. Glucose-induced abnormal egg-laying rate in Caenorhabditis
713 elegans. Bioscience, Biotechnology, and Biochemistry. 2016;80(7):1436-9.
714 46. Zheng J, Gao C, Wang M, Tran P, Mai N, Finley JW, et al. Lower Doses of Fructose Extend
715 Lifespan in Caenorhabditis elegans. Journal of Dietary Supplements. 2017;14(3):264-77.
716 47. Ke W, Reed JN, Yang C, Higgason N, Rayyan L, Wählby C, et al. Genes in human obesity loci are
717 causal obesity genes in C. elegans. PLOS Genetics. 2021;17(9):e1009736.
718 48. Gatrell L, Wilkins W, Rana P, Farris M. Glucose effects on polyglutamine-induced proteotoxic
719 stress in Caenorhabditis elegans. Biochemical and Biophysical Research Communications.
720 2020;522(3):709-15.
721 49. Beaudoin-Chabot C, Wang L, Celik C, Abdul Khalid AT-F, Thalappilly S, Xu S, et al. The unfolded
722 protein response reverses the effects of glucose on lifespan in chemically-sterilized C. elegans. Nature
723 Communications. 2022;13(1):5889.
724 50. Engstrom AK, Davis CD, Erichsen JL, Mondoux MA. Timing of High-glucose Diet in the C. elegans
725 Lifecycle Impacts Fertility Phenotypes. MicroPubl Biol. 2022;2022.
726 51. Mondoux MA, Love DC, Ghosh SK, Fukushige T, Bond M, Weerasinghe GR, et al. O-linked-N-
727 acetylglucosamine cycling and insulin signaling are required for the glucose stress response in
728 Caenorhabditis elegans. Genetics. 2011;188(2):369-82.
729 52. Wang X, Zhang L, Zhang L, Wang W, Wei S, Wang J, et al. Effects of excess sugars and lipids on
730 the growth and development of Caenorhabditis elegans. Genes & Nutrition. 2020;15(1):1.
731 53. Russell JW, Golovoy D, Vincent AM, Mahendru P, Olzmann JA, Mentzer A, et al. High glucose-
732 induced oxidative stress and mitochondrial dysfunction in neurons. The FASEB Journal.
733 2002;16(13):1738-48.
734 54. de Guzman ACV, Kang S, Kim EJ, Kim JH, Jang N, Cho JH, et al. High-Glucose Diet Attenuates the
735 Dopaminergic Neuronal Function in C. elegans, Leading to the Acceleration of the Aging Process. ACS
736 Omega. 2022;7(36):32339-48.
737 55. Gonzalez-Hunt CP, Luz AL, Ryde IT, Turner EA, Ilkayeva OR, Bhatt DP, et al. Multiple metabolic
738 changes mediate the response of Caenorhabditis elegans to the complex I inhibitor rotenone.
739 Toxicology. 2021;447:152630.
740 56. Sherer TB, Betarbet R, Testa CM, Seo BB, Richardson JR, Kim JH, et al. Mechanism of toxicity in
741 rotenone models of Parkinson's disease. J Neurosci. 2003;23(34):10756-64.
742 57. Sherer TB, Richardson JR, Testa CM, Seo BB, Panov AV, Yagi T, et al. Mechanism of toxicity of
743 pesticides acting at complex I: relevance to environmental etiologies of Parkinson's disease. J
744 Neurochem. 2007;100(6):1469-79.
745 58. McDonald PW, Hardie SL, Jessen TN, Carvelli L, Matthies DS, Blakely RD. Vigorous motor activity
746 in Caenorhabditis elegans requires efficient clearance of dopamine mediated by synaptic localization of
747 the dopamine transporter DAT-1. J Neurosci. 2007;27(51):14216-27.
748 59. Gabriel LR, Wu S, Kearney P, Bellvé KD, Standley C, Fogarty KE, et al. Dopamine Transporter
749 Endocytic Trafficking in Striatal Dopaminergic Neurons: Differential Dependence on Dynamin and the
750 Actin Cytoskeleton. The Journal of Neuroscience. 2013;33(45):17836-46.

751 60. Loder MK, Melikian HE. The dopamine transporter constitutively internalizes and recycles in a
752 protein kinase C-regulated manner in stably transfected PC12 cell lines. J Biol Chem.
753 2003;278(24):22168-74.
754 61. Geraldes P, King GL. Activation of protein kinase C isoforms and its impact on diabetic
755 complications. Circ Res. 2010;106(8):1319-31.
756 62. Campbell E, Schlappal A, Geller E, Castonguay TW. Chapter 19 - Fructose-Induced
757 Hypertriglyceridemia: A Review. In: Watson RR, editor. Nutrition in the Prevention and Treatment of
758 Abdominal Obesity. San Diego: Academic Press; 2014. p. 197-205.
759 63. Singh AR, Joshi S, Arya R, Kayastha AM, Srivastava KK, Tripathi LM, et al. Molecular cloning and
760 characterization of Brugia malayi hexokinase. Parasitology International. 2008;57(3):354-61.
761 64. Softic S, Meyer JG, Wang G-X, Gupta MK, Batista TM, Lauritzen HPMM, et al. Dietary Sugars
762 Alter Hepatic Fatty Acid Oxidation via Transcriptional and Post-translational Modifications of
763 Mitochondrial Proteins. Cell Metabolism. 2019;30(4):735-53.e4.
764 65. Su LJ, Mahabir S, Ellison G, McGuinn L, Reid B. Epigenetic Contributions to the Relationship
765 between Cancer and Dietary Intake of Nutrients, Bioactive Food Components, and Environmental
766 Toxicants. Frontiers in Genetics. 2012;2.
767 66. Mattsson JL. Mixtures in the real world: The importance of plant self-defense toxicants,
768 mycotoxins, and the human diet. Toxicology and Applied Pharmacology. 2007;223(2):125-32.
769 67. Mahaffey KR, Vanderveen JE. Nutrient-toxicant interactions: susceptible populations.
770 Environmental Health Perspectives. 1979;29:81-7.
771 68. Odland J, Deutch B, Hansen J, Burkow I. The importance of diet on exposure to and effects of
772 persistent organic pollutants on human health in the Arctic. Acta Paediatrica. 2003;92(11):1255-66.
773 69. Den Broeder MJ, Moester MJB, Kamstra JH, Cenijn PH, Davidoiu V, Kamminga LM, et al. Altered
774 Adipogenesis in Zebrafish Larvae Following High Fat Diet and Chemical Exposure Is Visualised by
775 Stimulated Raman Scattering Microscopy. International Journal of Molecular Sciences. 2017;18(4):894.
776 70. Branco AT, Lemos B. High Intake of Dietary Sugar Enhances Bisphenol A (BPA) Disruption and
777 Reveals Ribosome-Mediated Pathways of Toxicity. Genetics. 2014;197(1):147-57.
778 71. Liu J, Gupta RC, Goad JT, Karanth S, Pope C. Modulation of parathion toxicity by glucose feeding:
779 Is nitric oxide involved? Toxicology and Applied Pharmacology. 2007;219(2):106-13.
780 72. Sherwood DR, Butler JA, Kramer JM, Sternberg PW. FOS-1 promotes basement-membrane
781 removal during anchor-cell invasion in C. elegans. Cell. 2005;121(6):951-62.
782 73. Redemann S, Schloissnig S, Ernst S, Pozniakowsky A, Ayloo S, Hyman AA, et al. Codon
783 adaptation-based control of protein expression in C. elegans. Nat Methods. 2011;8(3):250-2.
784 74. Cothren SD, Meyer JN, Hartman JH. Blinded Visual Scoring of Images Using the Freely-available
785 Software Blinder. Bio Protoc. 2018;8(23).
786 75. Luz AL, Smith LL, Rooney JP, Meyer JN. Seahorse Xfe 24 Extracellular Flux Analyzer-Based
787 Analysis of Cellular Respiration in Caenorhabditis elegans. Curr Protoc Toxicol. 2015;66:25.7.1-.7.15.
788 76. Luz AL, Lagido C, Hirschey MD, Meyer JN. In Vivo Determination of Mitochondrial Function Using
789 Luciferase-Expressing Caenorhabditis elegans: Contribution of Oxidative Phosphorylation, Glycolysis, and
790 Fatty Acid Oxidation to Toxicant-Induced Dysfunction. Curr Protoc Toxicol. 2016;69:25.8.1-.8.2.

791

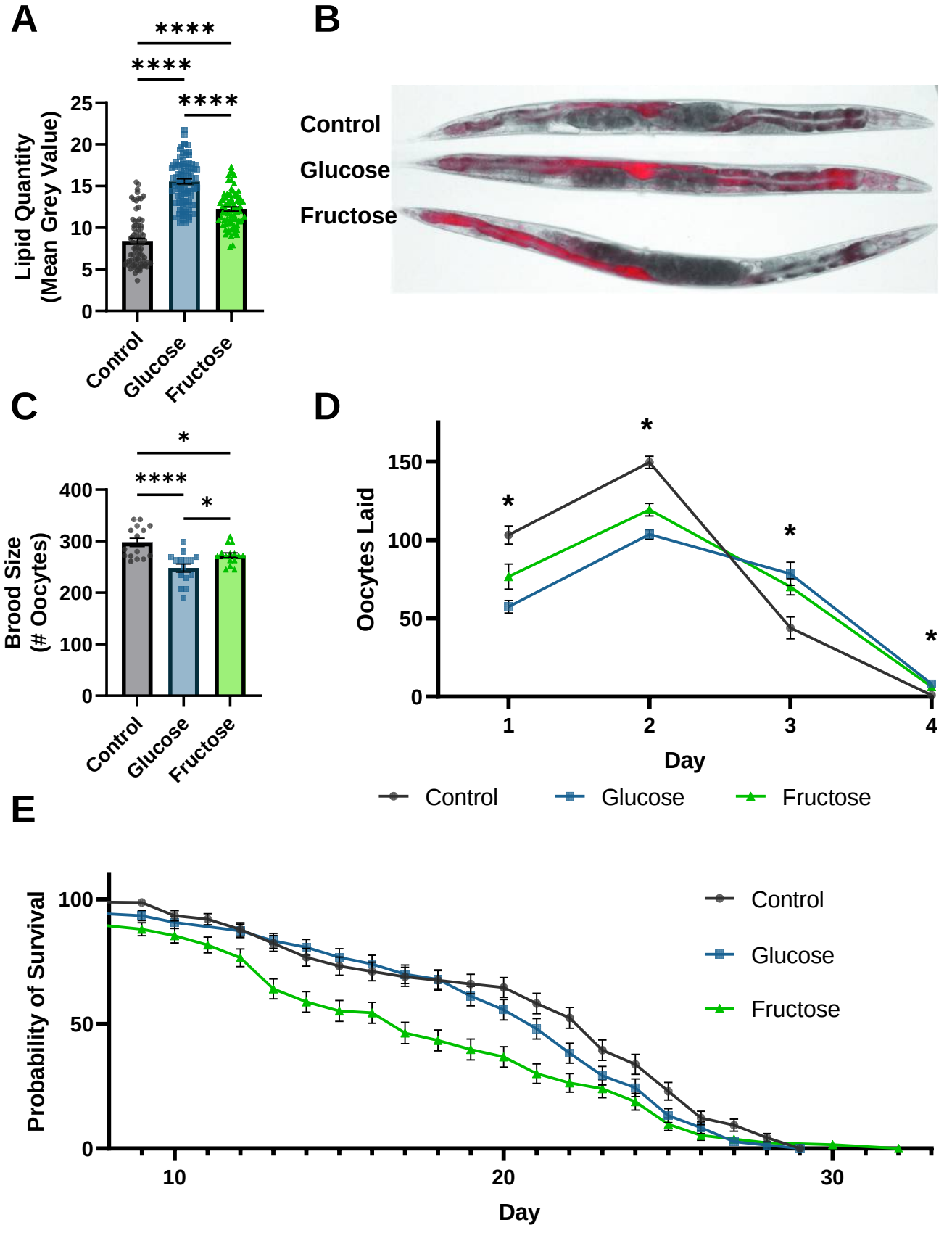
A
****
****
****
Lipid Quantity
(Mean Grey Value)
25
20
15
10
5
0
Control
Glucose
Fructose
B
Control
Glucose
Fructose
C
*
****
*
Brood Size
(# Oocytes)
400
300
200
100
0
Control
Glucose
Fructose
D
*
*
*
*
Oocytes Laid
150
100
50
0
1
2
3
4
Day
Control
Glucose
Fructose
E
Probability of Survival
100
50
0
10
20
30
Day
Control
Glucose
Fructose

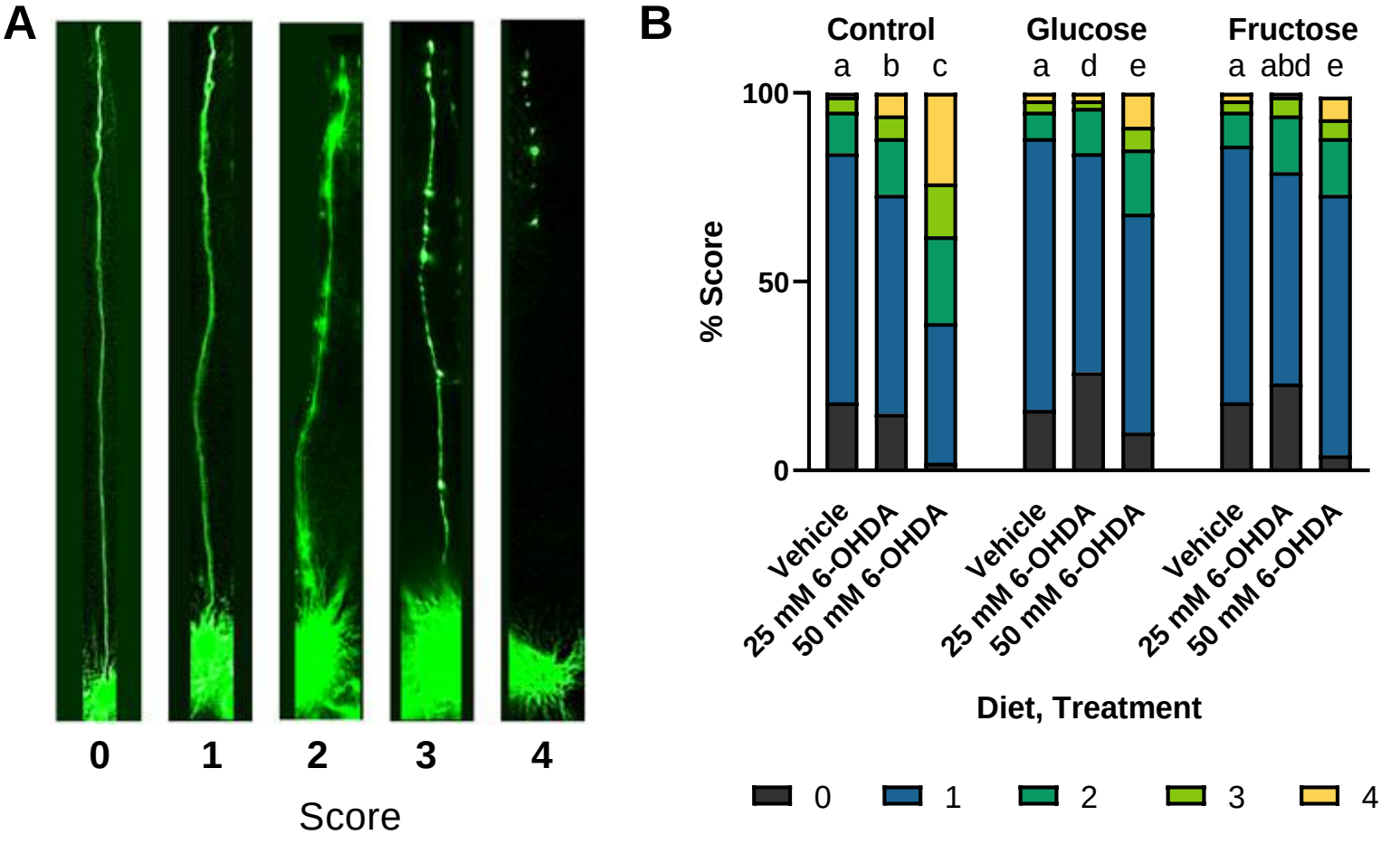
A
0
1
2
3
4
Score
B
Control
Glucose
Fructose
a b c
a d e
a abd e
100
50
0
% Score
Vehicle
25 mM 6-OHDA
50 mM 6-OHDA
Vehicle
25 mM 6-OHDA
50 mM 6-OHDA
Vehicle
25 mM 6-OHDA
50 mM 6-OHDA
Diet, Treatment
0
1
2
3
4

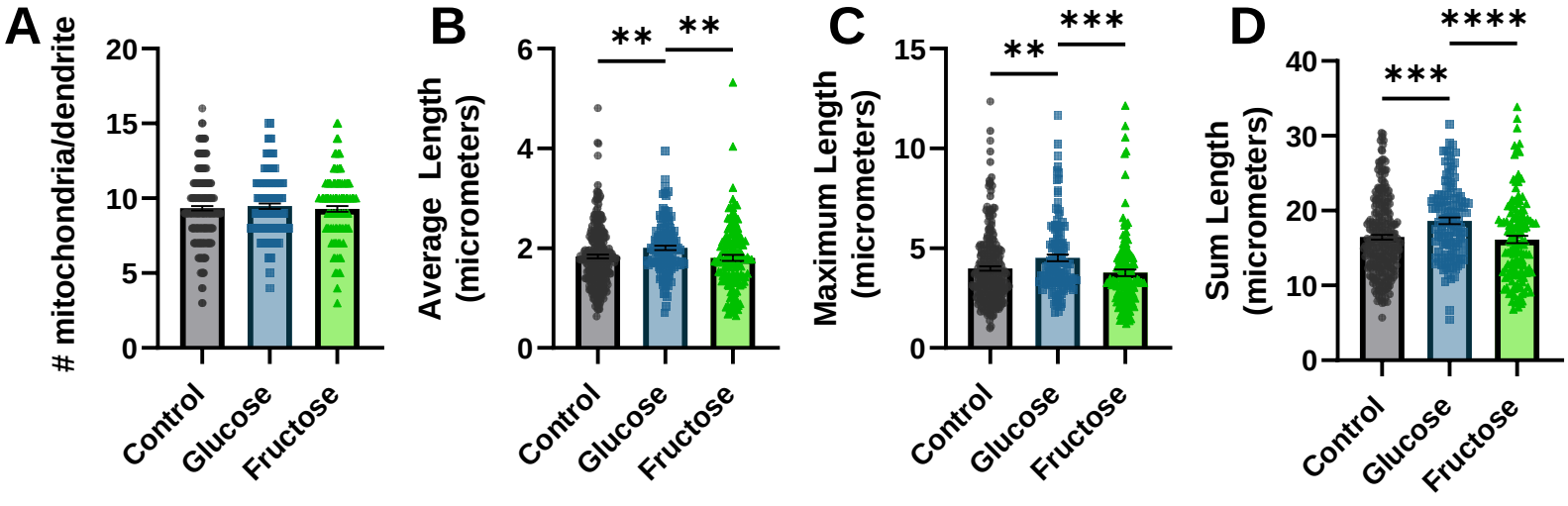
A
mitochondria/dendrite
20
15
10
5
0
Control
Glucose
Fructose
B
Average Length (micrometers)
6
4
2
0
**
**
Control
Glucose
Fructose
C
Maximum Length (micrometers)
15
10
5
0
**
***
Control
Glucose
Fructose
D
Sum Length (micrometers)
40
30
20
10
0
***
****
Control
Glucose
Fructose

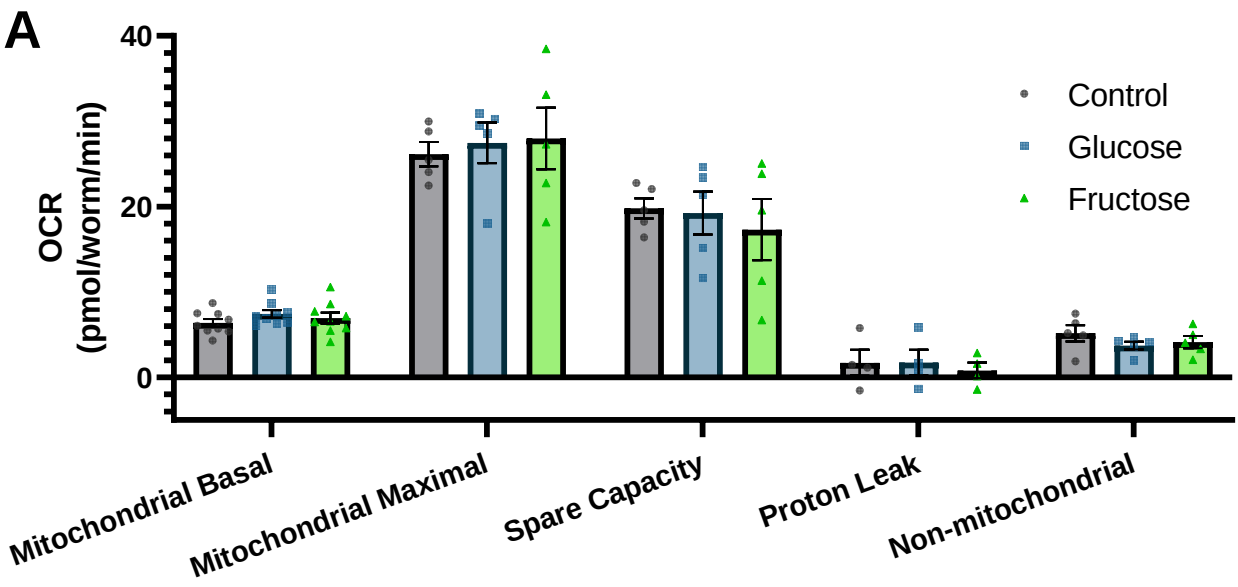
A
OCR
(pmol/worm/min)
40
20
0
Control
Glucose
Fructose
Mitochondrial Basal
Mitochondrial Maximal
Spare Capacity
Proton Leak
Non-mitochondrial

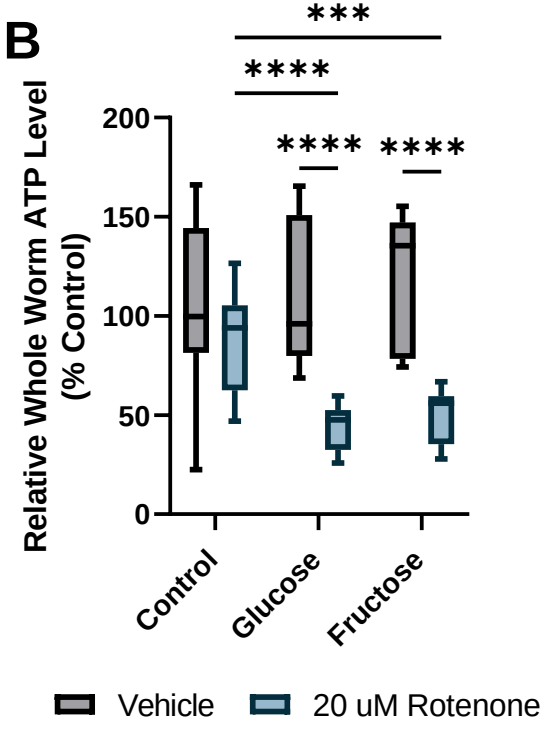
B
Relative Whole Worm ATP Level
(% Control)
200
150
100
50
0
***
****
****
****
Control
Glucose
Fructose
Vehicle
20 uM Rotenone

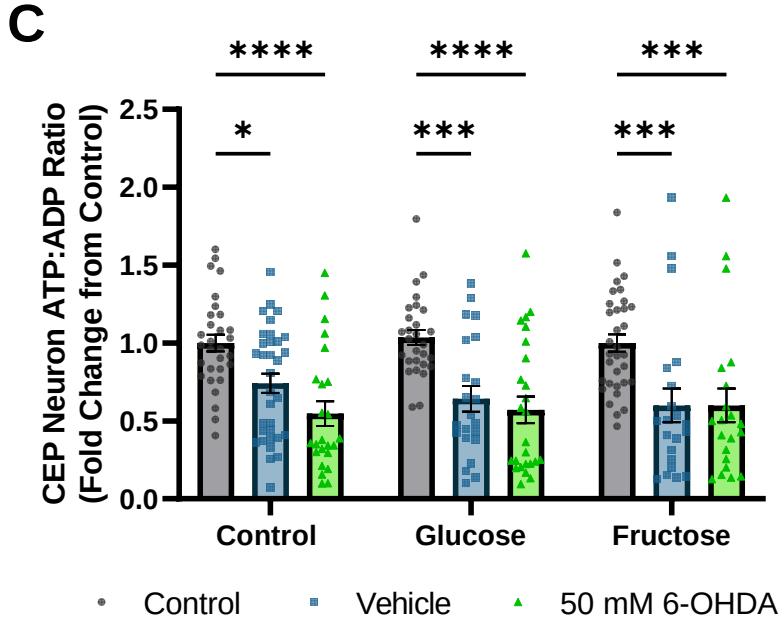
C
CEP Neuron ATP:ADP Ratio
(Fold Change from Control)
2.5
2.0
1.5
1.0
0.5
0.0
****
****
***
*
***
***
Control
Glucose
Fructose
Control
Vehicle
50 mM 6-OHDA

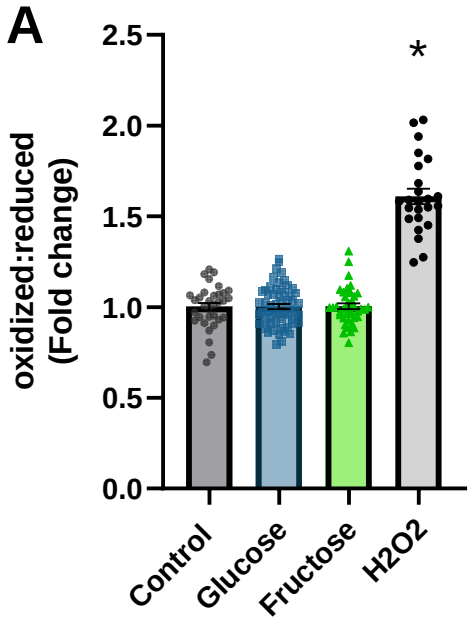
A
oxidized:reduced
(Fold change)
2.5
2.0
1.5
1.0
0.5
0.0
*
Control
Glucose
Fructose
H2O2

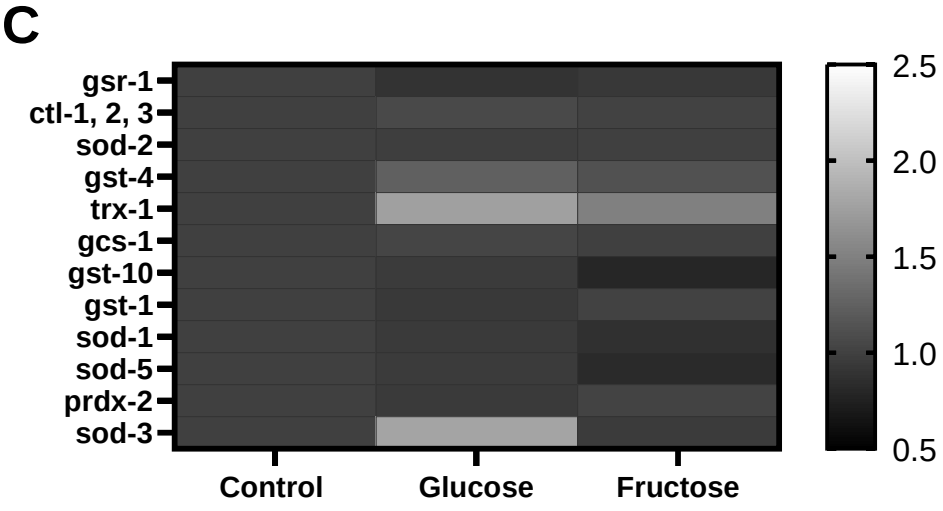
C
gsr-1
ctl-1, 2, 3
sod-2
gst-4
trx-1
gcs-1
gst-10
gst-1
sod-1
sod-5
prdx-2
sod-3
Control
Glucose
Fructose
2.5
2.0
1.5
1.0
0.5

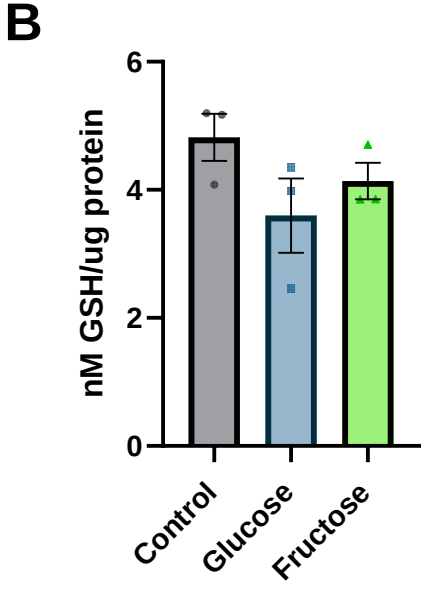
B
nM GSH/ug protein
6
4
2
0
Control
Glucose
Fructose

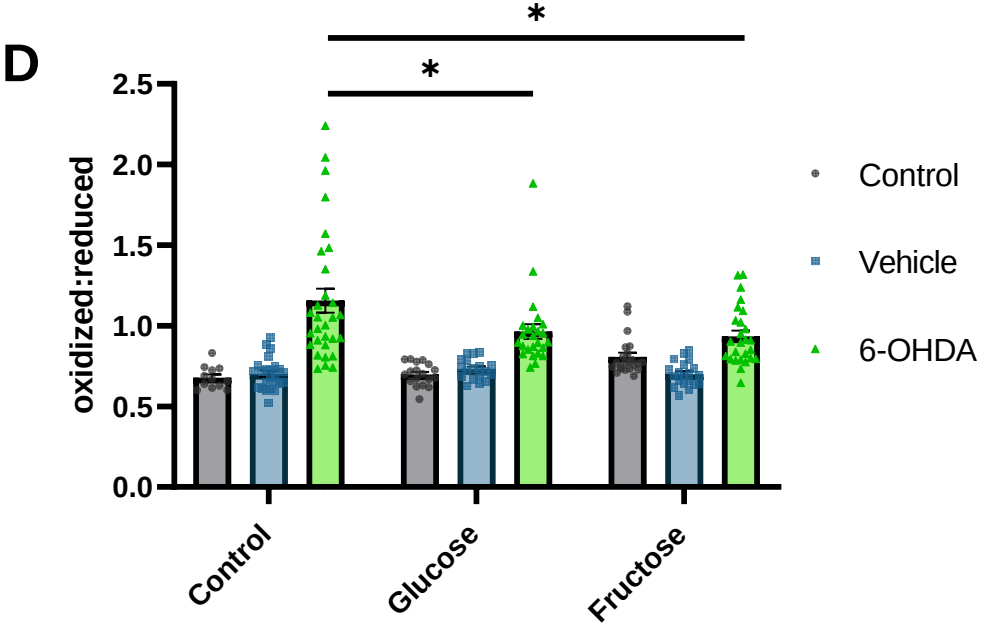
D
oxidized:reduced
2.5
2.0
1.5
1.0
0.5
0.0
*
*
Control
Glucose
Fructose
Control
Vehicle
6-OHDA

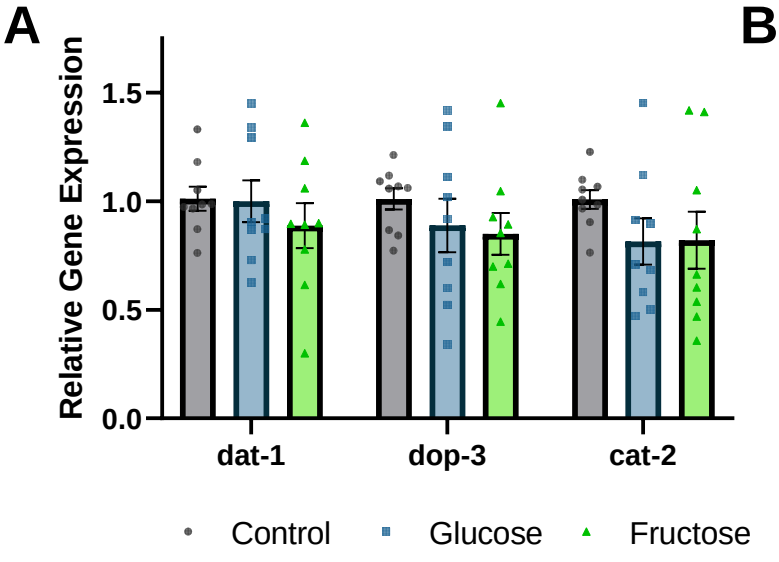
A
Relative Gene Expression
1.5
1.0
0.5
0.0
dat-1
dop-3
cat-2
Control
Glucose
Fructose

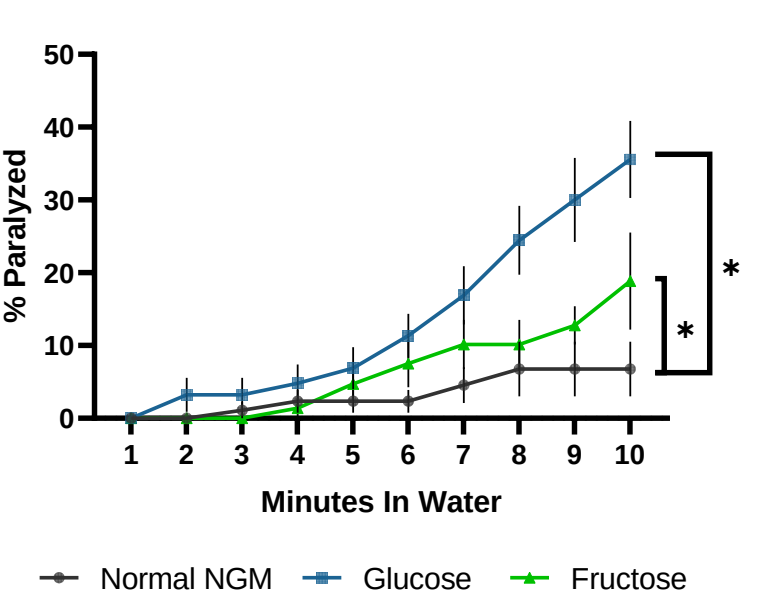
B
% Paralyzed
50
40
30
20
10
0
1
2
3
4
5
6
7
8
9
10
Minutes In Water
*
*
Normal NGM
Glucose
Fructose